Quantum Dots

DOI: 10.1002/anie.201008206

Chirality of Glutathione Surface Coating Affects the Cytotoxicity of Quantum Dots**

Yiye Li, Yunlong Zhou, Hai-Yan Wang, Sarah Perrett, Yuliang Zhao, Zhiyong Tang,* and Guangjun Nie**

Quantum dots (QDs) have been extensively investigated as fluorescent probes and are emerging as a new class of agents for biomedical imaging and diagnosis because of their broad absorption profiles, tunable emission wavelengths, and high photooxidation stability.[1–3] QDs consist of an inorganic core surrounded by an organic shell. Normally, different types of biomolecules, such as amino acids, DNA, or peptides, are used for the organic shell to facilitate water solubility and biocompatibility of the QDs. However, because the core may contain toxic heavy metals (e.g., Cd, Hg, Pb, and Zn), the potential cytotoxicity of QDs has been a major impediment to their widespread application.[4–6] It has therefore become critical to fully understand the interactions between QDs and living cells in order to develop nontoxic and biocompatible QDs for clinical use. Early studies have suggested that the release of core components, the generation of reactive oxygen species (ROS), and nonspecific binding to cellular membranes and intracellular proteins are the major mechanisms of the observed cytotoxic effects of QDs.[7–9] Despite a significant surge in the number of investigations into the cytotoxicity of QDs, there is currently only limited knowledge about the cytological and physiological mediators of these effects. Interestingly, recent data have suggested that the induction of autophagy by certain sizes of QDs could play an important role in their toxic actions.[10–12]

Autophagy is a metabolic process involved in protein and organelle degradation and plays key roles in maintaining cellular homeostasis and contributing to cellular defense.[13] It has been recognized as a third pathway of cell death, after apoptosis and necrosis, and is responsive to various physicopathological stimuli.[14] Recent work has shown that small QDs (< 10 nm) rather than those with larger sizes (40–50 nm) induce autophagy in cultured cells.[10,15] This size-dependent induction of autophagy has also been reported for other nanoparticles (NPs).[11,16,17] However, all the above studies focused on the effects of type and size of the NPs, while other factors that may induce autophagy remain unexplored.

Although many studies have demonstrated that surface modification of QDs with biomolecules endows them with various biological functionalities, the impact on living organisms of the chirality of the surface biomolecules has been largely neglected. Chirality is an important phenomenon in living systems and nearly all biological polymers must be homochiral to function. For example, all amino acids in proteins are "left-handed", whereas all sugars in DNA and RNA are "right-handed".[18] Different chiral properties of biomolecules may determine their ability to interact with other biomolecules and thereby modulate a range of downstream processes. More recently, several attempts to develop chiral QDs with optical activities using different chiral stabilizers have been reported.[19–22]

Herein, the effects of QDs capped with different chiral forms of the tripeptide glutathione (GSH) on cytotoxicity and induction of autophagy were examined. Two different sizes of cadmium telluride (CdTe) QDs coated with either L-GSH (L-GSH-QDs) or D-GSH (D-GSH-QDs) were found to show dose-dependent cytotoxicity and to significantly increase the levels of autophagic vacuoles. The activation of autophagy was chirality-dependent, with L-GSH-QDs being more effective than D-GSH-QDs. The ability of QDs to induce cell death was correlated with their ability to induce autophagy. This chirality-associated regulation of cellular metabolism and cytotoxicity highlights the important role of the conformation of the stabilizers, and has important implications for the design of novel QDs with enhanced optical properties and reduced or no toxicity.

In this study, negatively charged water-soluble CdTe QDs were synthesized according to the Rogach–Weller method[23] and coated with different chiral forms of GSH as stabilizers (Figure 1a). To clearly understand the chirality effect, two series of QDs were prepared. Group 1 comprised small-sized

[*] Y. Li,[+] Prof. Y. Zhao, Prof. G. Nie
CAS Key Laboratory for Biological Effects of Nanomaterials & Nanosafety, National Center for Nanoscience and Technology
11 Beiyijie, Zhongguancun, Beijing 100190 (China)
E-mail: niegj@nanoctr.cn
H. Y. Wang, Prof. S. Perrett
National Laboratory of Biomacromolecules, Institute of Biophysics
Chinese Academy of Sciences
15 Datun Road, Chaoyang District, Beijing 100101 (China)
Y. Zhou,[+] Prof. Z. Tang
Laboratory of Nanomaterials
National Center for Nanoscience and Technology, Beijing (China)
E-mail: zytang@nanoctr.cn
Prof. Y. Zhao
CAS Key Laboratory for Biological Effects of Nanomaterials & Nanosafety, Institute of High Energy Physics
Chinese Academy of Sciences (China)
E-mail: zhaoyuliang@ihep.ac.cn
[+] These authors contributed equally to this work.

[**] This work was supported by grants from MOST 973 (2011CB9334001, 2010CB933600, 2009CB930401), 863 (2009AA03Z335), and the NSFC (10979011, 30900278, 20973047, 21025310, 10525524, 31070656). G.N. and Z.T. gratefully acknowledge the support of the CAS Hundred Talents Program. We thank Prof. G. Anderson for reviewing the manuscript. pEGFP-LC3 plasmid was a gift from Prof. N. Mizushima and Prof. C. Y. Jiang.

Supporting information for this article is available on the WWW under http://dx.doi.org/10.1002/anie.201008206.

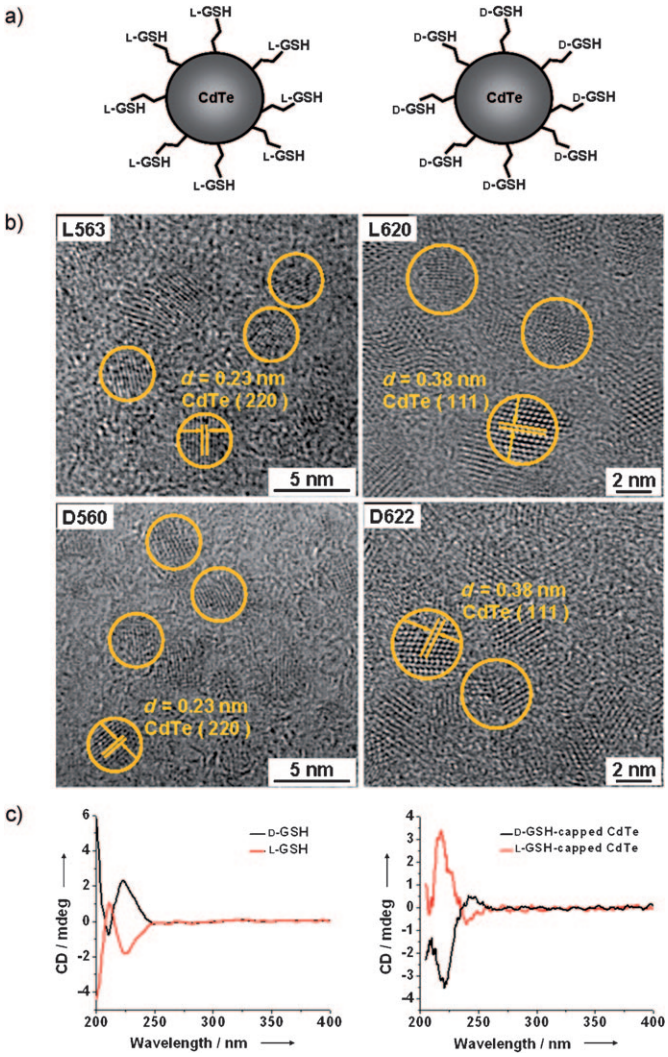

Figure 1. Characterization of D- and L-GSH-QDs. a) Schematic diagram of L- (left) and D-GSH-QDs (right). b) HRTEM images of D- and L-GSH-QDs of different sizes. The spherical QDs are marked by circles with a distance of the lattice spacing (220) or (111) of zinc blende CdTe, as indicated. c) CD spectra of L- and D-GSH and the L- and D-GSH-QDs.

QDs with green fluorescence (L563 QDs, L-GSH capped, emission maximum (λ_{em}) = 563 nm; D560 QDs, D-GSH capped, λ_{em} = 560 nm). Group 2 consisted of large-sized QDs with red fluorescence (L620 QDs, L-GSH capped, λ_{em} = 620 nm; D622 QDs, D-GSH capped, λ_{em} = 622 nm; see Figure S1 in the Supporting Information). Characterization by X-ray diffraction (XRD) analysis showed that QDs have typical zinc blende crystal structures (Figure S2 in the Supporting Information).[24] High-resolution transmission electron microscopy (HRTEM) indicated that all QDs are approximately spherical in shape. The lattice spacing of the (220) plane for D560 and L563 QDs showed a distance of 0.23 nm, and of the (111) plane for D622 and L620 QDs a distance of 0.38 nm (Figure 1b).

Table 1 summarizes the physical properties of the QDs. L- and D-GSH-QDs have the same size, surface charge, and fluorescence properties. The sizes of L563 and D560 QDs are about 3.2 nm, while L620 and D622 QDs are around 4.2 nm. The only difference between these two types of QDs is their chirality. L563 and D560 QDs showed essentially mirror-image circular dichroism (CD) spectra in the region of 200 to 300 nm (Figure 1c). Similar CD characteristics were observed for L620 and D622 QDs (data not shown). It is also of note that, compared with chiral QDs, free L- and D-GSH molecules also show mirror-image CD spectra, but the signals are reversed (Figure 1c). Such reversal of CD signals after molecule adsorption onto the QD surface has been reported previously.[19] All the QDs, regardless of size or chirality, were found to be stable and no significant degree of aggregation or decomposition was observed after storage in phosphate-buffered saline (PBS) solution for two days (Figure S3 in the Supporting Information).

Table 1: Physicochemical properties of CdTe QDs.

CdTe	Surface modification	Diameter[a] [nm]	ζ-potential [mv]	λ_{em}[b] [nm]	Quantum yield
L563	L-GSH	3.2	−50	563	0.44
L620	L-GSH	4.2	−51	620	0.54
D560	D-GSH	3.2	−47	560	0.53
D622	D-GSH	4.2	−54	622	0.46

[a] The diameters of the QDs were the average of at least 100 measurements in the TEM images. [b] Emission maximum.

To explore the different biochemical effects of L- and D-GSH-QDs, we first compared their effects on cell viability in human hepatoma HepG2 cells. As shown in Figure 2a(1), both L- and D-GSH-QDs showed concentration- and chirality-dependent cytotoxicity, with L-GSH-QDs showing greater cytotoxicity for a given concentration. We then compared their effects on induction of autophagy. Relative to controls, all four QDs tested triggered conversion of microtubule-associated protein light chain 3 (LC3)-I to LC3-II, the best-characterized marker of autophagy[25] (Figure 2a(2)). This activation of autophagy was chirality-dependent, with L-GSH-QDs inducing more dramatic autophagy than D-GSH-QDs, regardless of QD size. Size-dependent effects were also observed, with L563 QDs demonstrating the strongest effects and D622 QDs showing the weakest effects on stimulation of autophagy (Figure 2a(2)).

To study the relationship between dosage of QDs and ability to induce autophagy, different concentrations of QDs were used to measure their ability to induce autophagy. As shown in Figure S4 in the Supporting Information, induction of autophagy by QDs was observed under lower-concentration treatment (10 and 20 nM). It was also chirality-dependent and L-GSH-QDs stimulated more LC3-II expression. However, lower doses showed less profound differences between the two types of QDs. To further confirm induction of autophagy as being a chirality-dependent process, we examined the effects of QDs on HepG2 cells stably overexpressing LC3-EGFP (EGFP = enhanced green fluorescent protein). Fluorescence microscopy showed that all QDs induced LC3-EGFP aggregation in HepG2 cells, although the effect was very weak for D622 QDs (Figure 2b). As a positive control, amiodarone hydrochloride (AH) significantly induced autophagy.[26]

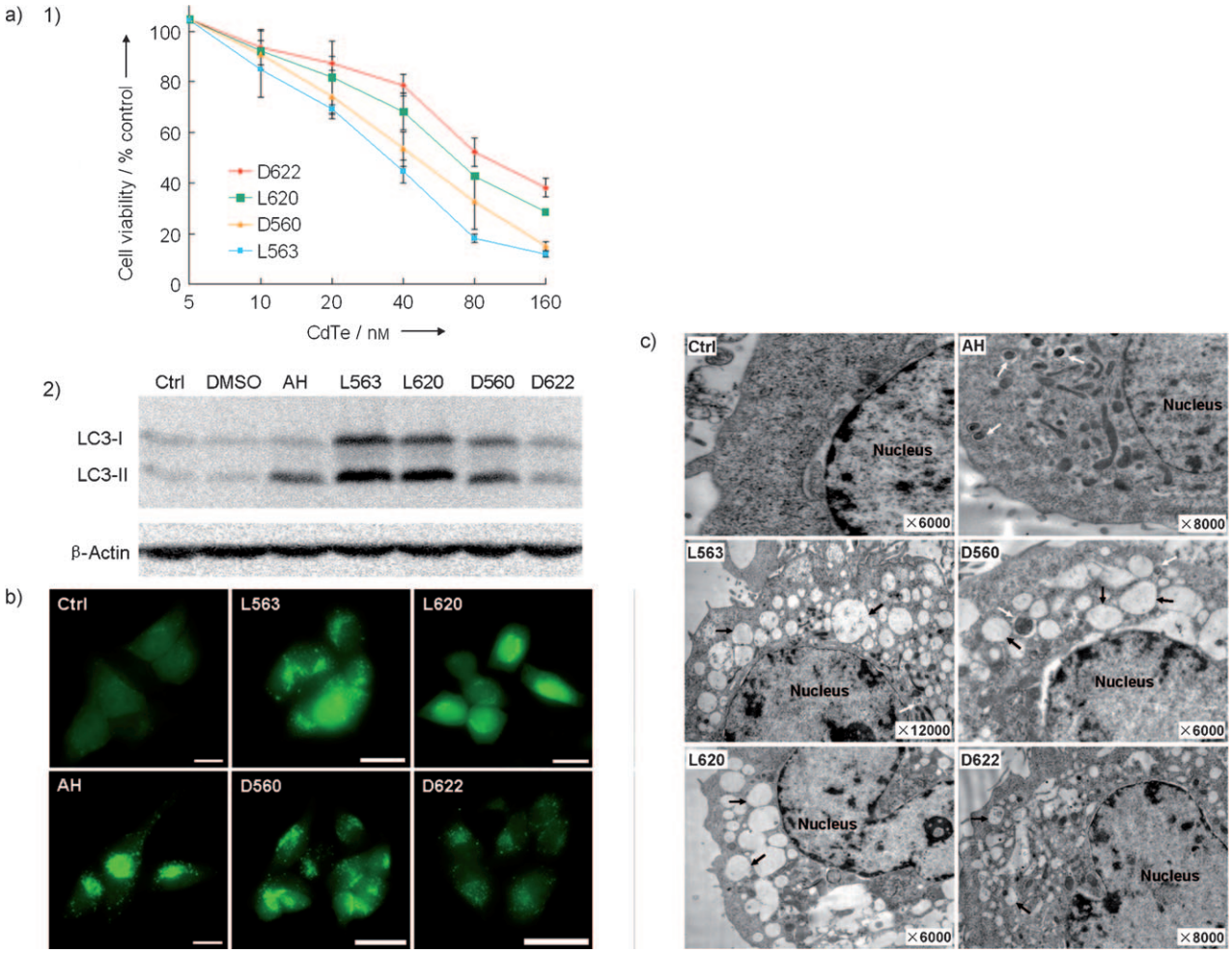

Figure 2. Induction of cell death and accumulation of autophagic vacuoles by QDs are chirality-dependent. a) 1) Concentration- and chirality-dependent cytotoxicity of QDs. 2) L-GSH-capped QDs had more profound effects on the induction of autophagy than D-GSH-QDs (40 nM). b) Fluorescence microscopy images of LC3-EGFP in HepG2 cells stably overexpressing LC3-EGFP following QD treatment. Scale bars: 25 μm. c) TEM images of HepG2 cells treated with QDs for 24 h. AH was used as a positive control and autophagic vacuoles, consisting of double-layered membranes containing cellular debris, are indicated by white arrows. QD-triggered autophagic cell death was characterized by numerous large vacuoles within the cytoplasm (black arrows).

To more precisely define the morphological changes and cellular vacuole formation accompanying QD treatment, HepG2 cells exposed to QDs for 24 hours were examined by TEM. In comparison with untreated controls, a number of autophagosomes containing internalized cytoplasmic debris were observed as darkly stained granular inclusions in AH-treated cells (Figure 2c, white arrows). The most striking feature of the QD-treated cells was the large number of empty vacuoles appearing in the cytoplasm (Figure 2c, black arrows). Some QD-treated cells also showed autophagic vacuoles bounded by membrane bilayers or dark granular aggregates, which most likely represent the accumulation of QDs (Figure 2c). D622 QDs were less effective at accumulating vacuole formation than the other three types of QDs. These morphological observations on the formation of large numbers of autophagic vacuoles are consistent with increases in LC3-II expression and LC3-EGFP fluorescence intensity (Figures 2a(2) and b).

Autophagic cell death is a cytoprotective mechanism that responds to stress conditions and allows the living organisms to adapt to environmental and developmental changes.[27] As shown in Figure 2c, numerous large vacuoles appeared in the cytoplasm of QD-treated cells, features of autophagic cell death. To determine whether the accumulation of autophagic vacuoles was associated with QD-dependent cytotoxicity, quantitative measurements of cell viability after QD and autophagy inhibitor treatment were carried out. HepG2 cell viability dramatically decreased in L563-, L620-, and D560-treated cells after 12 and 24 hours of incubation (Figures 3a and b, respectively), consistent with the results of Figure 2a(1). For QDs with similar diameters, L-GSH-coated QDs were more cytotoxic than D-GSH-modified QDs and this pattern parallels the ability of QDs to induce autophagy. This correlation indicates that the cell death induced by the QDs may be mediated, at least partially, by an autophagy-dependent mechanism. To examine this hypothesis, we pretreated the cells with the autophagy inhibitor 3-methyladenine (3MA; Figures 3a and b). 3MA pretreatment significantly rescued cells, although it did not completely block QD-induced cell death, especially in cells treated with L563, L620,

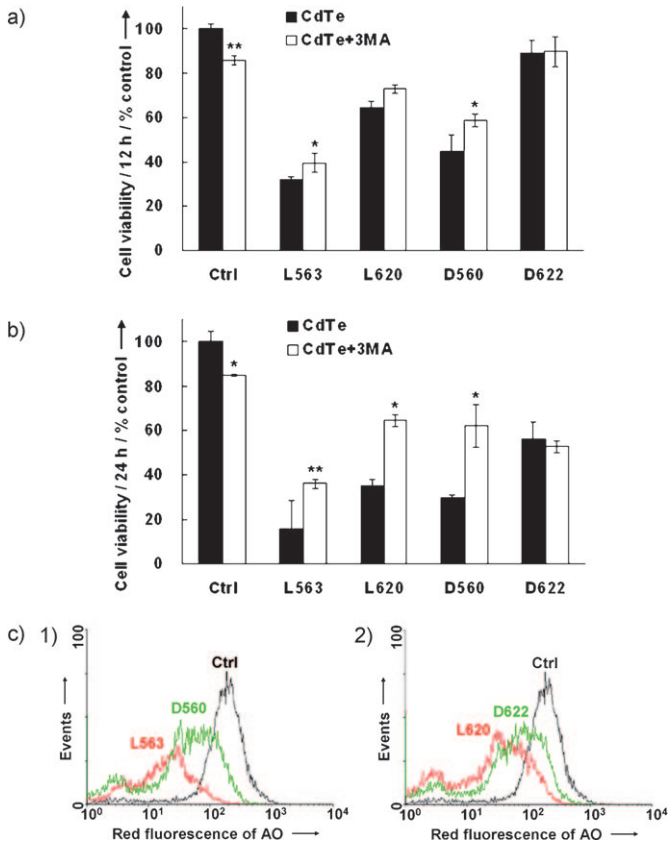

Figure 3. QD-induced cytotoxicity is chirality-dependent and is decreased by an inhibitor of autophagy. HepG2 cell viability was measured after a) 12 or b) 24 h of QD treatment. In some studies, cells were pretreated with 3 mM 3MA for 12 h. $*p < 0.05$ and $**p < 0.01$ compared to the cells without 3MA pretreatment. c) QDs decreased lysosome stability in HepG2 cells. Representative histograms show the effects of both 1) 560 QDs and 2) 620 QDs on lysosomal stability.

and D560 QDs. The effects were most noticeable after 24 hours of treatment with the QDs. For D622 QD-treated cells, no changes in cell viability were observed after either 12 or 24 hours of incubation with 3MA. The fact that 3MA had no effect on the cell viability in D622 QD-treated cells (Figures 3a and b) and did not completely block cell death induced by the other QDs may indicate that, in addition to autophagy-dependent cell death, QDs may be killing cells through other mechanisms.

Lysosomes play an important role in autophagy and are believed to be the key organelles involved in autophagy-mediated cell death.[13] The fate of NPs in lysosomes has been discussed recently.[28] To determine whether QDs could interfere with lysosome function, the integrity of lysosomal membranes was assessed by using flow cytometry to examine the release of acridine orange (AO) from lysosomes into the cytosol (Figure 3c). For QDs with the same sizes, the degree of loss of the AO fluorescence signal was greater in cells treated with L-GSH-QDs than in those treated with D-GSH-QDs (Figure 3c(1) and (2)). The stability of lysosomal membranes in the cells after treatment with GSH-QDs also correlated with the induction of autophagy. Furthermore, we observed that the pH of lysosomes was affected by QD treatment (Figure S5 in the Supporting Information). After incubation with L563 and D560 QDs for 24 hours, HepG2 cells were labeled with LysoSensor, followed by measurement of its fluorescence intensity. Cells treated with both types of QDs exhibited a pH-dependent increase in green fluorescence intensity of LysoSensor, which indicated that the lysosomal pH was decreased.

To assess the cellular distribution of QDs, we treated HepG2 and RAW264.7 cells with 20 nM L620 QDs. After 4 hours of treatment, both cell lines showed red punctuated fluorescence in the cytoplasm, but no signal was detected in the nuclei. After 24 hours of treatment, L620 QDs were distributed throughout the cytoplasm of both cell types, which indicated that more QDs were acquired by the cells after 24 hours of labeling (Figure 4a). The TEM studies (Figure 2c) also supported the fluorescence microscopy analysis and confirmed that QDs are taken up by the cells and are distributed mainly in the cytoplasm.

Since the differential biological effects of QDs could also be linked to their differential cellular uptake, quantitative measurements of QD cellular uptake were carried out by measuring the elemental cadmium (Cd) content using inductively coupled plasma–mass spectrometry (ICP-MS[29]; Figure 4b). Similar levels of Cd in equal numbers of cells confirmed that the QDs with similar sizes but different chirality had comparable cellular uptake. Therefore, the observed differential effects of QD chirality on the accumulation of autophagic vacuoles and associated cytotoxicity are dependent mainly, if not entirely, on their interaction with autophagy machinery, rather than differential cellular uptake.

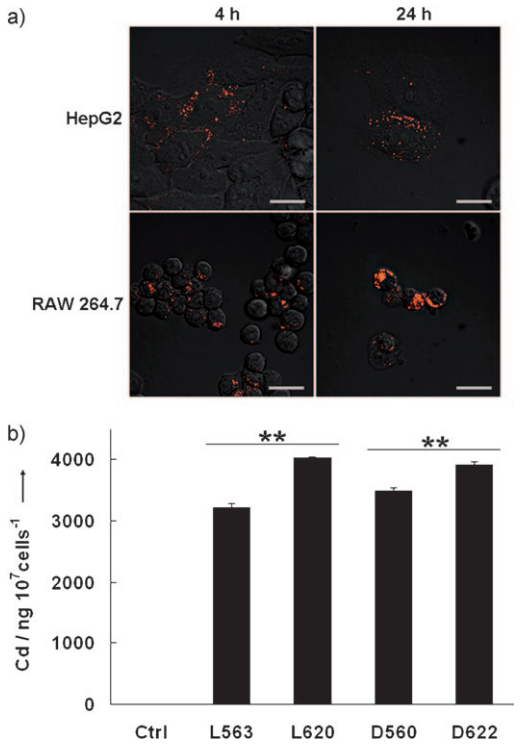

Figure 4. Cellular uptake of GSH-QDs. a) Confocal images of HepG2 and RAW264.7 cells treated with L620 QDs for 4 or 24 h. Scale bars: 20 μm. b) Quantification of cadmium levels by ICP-MS in 1×10^7 HepG2 cells treated with QDs for 24 h.

At the same time, it was found that larger QDs were more readily taken up by the cells than the smaller QDs, regardless of their surface chirality. Considering this, as well as the fact that multiple mechanisms associated with QD cytotoxicity may exist, the intracellular doses of the QDs may also play a role in determining their cytotoxicity.

To discriminate the difference between the D- and L-GSH, especially their different biological functions, we carried out a coupled enzymatic assay to address whether D-GSH is biologically active. Our study showed that D-GSH could not be used as an enzymatic substrate for glutathione reductase (GR) or the glutaredoxin, Ure2[30] (Figure S6 in the Supporting Information). Further, D-GSH did not inhibit or interfere with L-GSH in the same enzymatic reactions (data not shown), which suggests that D-GSH does not compete with L-GSH for binding to the active site.

It is possible that L-GSH (or other thiol-containing molecules) inside cells could replace the D-GSH stabilizer through a surface exchange reaction.[28] A similar surface exchange reaction has been observed in aqueous solution,[31] although it is not clear if this reaction happens in cells. Our study demonstrates that free L-GSH (1 mM) led to only a limited decline in the CD signal of D-GSH-QDs (Figure S7 in the Supporting Information). The intracellular concentration of L-GSH in HepG2 cells, as used in this study, is in the range of 0.1 to 0.25 mM (personal communication, S. T. Stern, Nanotechnology Characterization Lab, NCI). Therefore, although the surface exchange reaction may indeed occur to some extent, it should not greatly affect the chirality of QDs under the conditions of our experiments. On the other hand, the abundance of L-GSH, and the absence of D-GSH in biological systems, may affect the shell degradation of QDs. It would be expected that GSH-coated QDs will prefer to accommodate GSH of the same enantiomer. Where only one enantiomer is available, this preference would then affect the relative thermodynamic stability of the QDs coated by L-GSH or D-GSH. Consistent with this, D-GSH-QDs showed a faster decrease in their fluorescence than L-GSH-QDs in biomimetic fluid containing 0.25 mM L-GSH (Figure S8 in the Supporting Information).

In summary, this work provides new insights into QD-induced cellular injury by demonstrating differential toxicity associated with the chirality of GSH coating. QDs coated with D-GSH, the nonbiologically active form of GSH, showed less cytotoxicity than L-GSH-coated QDs. Identification of this chirality-dependent cytotoxicity of QDs provides important insight for designing more "inert" surface coatings using biomolecules and may open a new avenue for further development of QDs for biomedical imaging. Furthermore, the accumulation of autophagic vacuoles by QDs may also suggest a general mechanism for cytotoxicity associated with NP exposure, which may mimic a cytoprotective mechanism when cells encounter exposure to foreign particles, such as viruses or bacteria.

Received: December 27, 2010
Revised: March 21, 2011
Published online: May 12, 2011

Keywords: autophagy · chirality · cytotoxicity · fluorescence · quantum dots

[1] W. Chan, S. Nie, *Science* **1998**, *281*, 2016 – 2018.
[2] I. Medintz, H. Uyeda, E. Goldman, H. Mattoussi, *Nat. Mater.* **2005**, *4*, 435 – 446.
[3] A. M. Smith, M. C. Mancini, S. Nie, *Nat. Nanotechnol.* **2009**, *4*, 710 – 711.
[4] N. Singh, B. Manshian, G. J. Jenkins, S. M. Griffiths, P. M. Williams, T. G. Maffeis, C. J. Wright, S. H. Doak, *Biomaterials* **2009**, *30*, 3891 – 3914.
[5] A. Nel, T. Xia, L. Madler, N. Li, *Science* **2006**, *311*, 622 – 627.
[6] W. J. Stark, *Angew. Chem.* **2011**, *123*, 1276 – 1293; *Angew. Chem. Int. Ed.* **2011**, *50*, 1242 – 1258.
[7] A. Nel, L. Madler, D. Velegol, T. Xia, E. Hoek, P. Somasundaran, F. Klaessig, V. Castranova, M. Thompson, *Nat. Mater.* **2009**, *8*, 543 – 557.
[8] C. Kirchner, T. Liedl, S. Kudera, T. Pellegrino, A. Munoz Javier, H. E. Gaub, S. Stolzle, N. Fertig, W. J. Parak, *Nano Lett.* **2005**, *5*, 331 – 338.
[9] T. J. Brunner, P. Wick, P. Manser, P. Spohn, R. N. Grass, L. K. Limbach, A. Bruinink, W. J. Stark, *Environ. Sci. Technol.* **2006**, *40*, 4374 – 4381.
[10] O. Seleverstov et al., see the Supporting Information.
[11] O. Zabirnyk, M. Yezhelyev, O. Seleverstov, *Autophagy* **2007**, *3*, 278 – 281.
[12] S. T. Stern, D. N. Johnson, *Autophagy* **2008**, *4*, 1097 – 1100.
[13] N. Mizushima, B. Levine, A. Cuervo, D. Klionsky, *Nature* **2008**, *451*, 1069 – 1075.
[14] Y. Tsujimoto, S. Shimizu, *Cell Death Differ.* **2005**, *12*, 1528 – 1534.
[15] O. Seleverstov, J. M. Phang, O. Zabirnyk, *Methods Enzymol.* **2009**, *452*, 277 – 296.
[16] H. Yamawaki, N. Iwai, *Am. J. Physiol. Cell Physiol.* **2006**, *290*, C1495 – 1502.
[17] C. Li et al., see the Supporting Information.
[18] W. Bonner, *Origin Life Evol. Biosph.* **1995**, *25*, 175 – 190.
[19] M. Moloney, Y. Gun'ko, J. Kelly, *Chem. Commun.* **2007**, 3900 – 3902.
[20] S. D. Elliott, M. P. Moloney, Y. K. Gun'ko, *Nano Lett.* **2008**, *8*, 2452 – 2457.
[21] T. Nakashima, Y. Kobayashi, T. Kawai, *J. Am. Chem. Soc.* **2009**, *131*, 10342 – 10343.
[22] Y. Zhou, M. Yang, K. Sun, Z. Tang, N. A. Kotov, *J. Am. Chem. Soc.* **2010**, *132*, 6006 – 6013.
[23] N. Gaponik, D. Talapin, A. Rogach, K. Hoppe, E. Shevchenko, A. Kornowski, A. Eychmüller, H. Weller, *J. Phys. Chem. B* **2002**, *106*, 7177 – 7185.
[24] R. Viswanatha, S. Sapra, T. Saha-Dasgupta, D. Sarma, *Phys. Rev. B* **2005**, *72*, 45 333.
[25] N. Mizushima, *Cell. Physiol. Biochem.* **2004**, *36*, 2491 – 2502.
[26] L. Zhang et al., see the Supporting Information.
[27] F. Cecconi, B. Levine, *Dev. Cell* **2008**, *15*, 344 – 357.
[28] P. Podsiadlo, V. A. Sinani, J. H. Bahng, N. W. Kam, J. Lee, N. A. Kotov, *Langmuir* **2008**, *24*, 568 – 574.
[29] L. K. Limbach, Y. Li, R. N. Grass, T. J. Brunner, M. A. Hintermann, M. Muller, D. Gunther, W. J. Stark, *Environ. Sci. Technol.* **2005**, *39*, 9370 – 9376.
[30] Z. R. Zhang, S. Perrett, *J. Biol. Chem.* **2009**, *284*, 14058 – 14067.
[31] V. Sinani, P. Podsiadlo, J. Lee, N. Kotov, *Int. J. Nanotechnol.* **2007**, *4*, 239 – 251.

